TURBULENT HEATING OF THE DISTANT SOLAR WIND BY INTERSTELLAR PICKUP PROTONS IN A DECELERATING FLOW

The Astrophysical Journal, 719:716–721, 2010 August 10 doi:10.1088/0004-637X/719/1/716

TURBULENT HEATING OF THE DISTANT SOLAR WIND BY INTERSTELLAR PICKUP PROTONS IN A DECELERATING FLOW

Philip A. Isenberg[1], Charles W. Smith[1], William H. Matthaeus[2], and John D. Richardson[3]
[1] Institute for the Study of Earth, Oceans, and Space, University of New Hampshire, Durham, NH 03824, USA
[2] Bartol Research Institute, University of Delaware, Newark, DE 19716, USA
[3] Center for Space Research, Massachusetts Institute of Technology, Cambridge, MA 02139, USA
Received 2010 May 3; accepted 2010 June 13; published 2010 July 22

ABSTRACT

Previous models of solar wind heating by interstellar pickup proton-driven turbulence have assumed that the wind speed is a constant in heliocentric radial position. However, the same pickup process, which is taken to provide the turbulent energy, must also decelerate the wind. In this paper, we extend our phenomenological turbulence model to include variable wind speed, and then incorporate the deceleration due to interstellar pickup protons into the model. We compare the model results with plasma and field data from *Voyager 2*, taking this opportunity to present an extended and improved data set of proton core temperature, magnetic field fluctuation intensity, and correlation length along the *Voyager* trajectory. A particular motivation for including the solar wind deceleration in this model is the expectation that a slower wind would reduce the resulting proton core temperature in the region beyond ∼60 AU, where the previous model predictions were higher than the observed values. However, we find instead that the deceleration of the steady-state wind increases the energy input to the turbulence, causing even higher temperatures in that region. The increased heating is shown to result from the larger values of the ratio of Alfvén speed to solar wind speed that develop in the decelerating wind.

Key words: solar wind – turbulence

1. INTRODUCTION

Interstellar pickup ions originate as neutral atoms in the local interstellar medium, which then penetrate into the region of supersonic solar wind as a result of the slow relative motion of the heliosphere through this medium. When one of these atoms is ionized through an encounter with a solar UV photon or a charge-exchange collision with a solar wind ion, it suddenly appears in the reference frame of the solar wind plasma as an energetic charged particle traveling toward the Sun at the solar wind speed, V_{sw}. These new ions immediately gyrate about the local magnetic field, forming a ring–beam distribution which is unstable to the generation of MHD waves (Wu & Davidson 1972; Lee & Ip 1987; Bogdan et al. 1991). They subsequently scatter to a stable, nearly isotropic shell in velocity space through the cyclotron resonant interaction with the self-generated and ambient waves. At this point, these particles are comoving with the bulk solar wind and are said to be "picked up." As they accumulate in the outflowing solar wind, they form a distinct energetic population of the plasma (see Zank 1999 for an excellent and extensive review).

The primary component of the inflowing neutral gas is hydrogen, with a density at the solar wind termination shock of $N_o \sim 0.1$ cm^{-3} (Gloeckler et al. 1997; Bzowski et al. 2009). The resulting pickup protons come to dominate the internal thermal energy of the plasma far from the Sun and are responsible for large-scale observable effects at heliocentric distances $r > 20$ AU. For instance, the momentum loading by the pickup of these particles causes a continual slowing of the solar wind speed (Wallis 1971; Holzer 1972; Isenberg 1986; Lee 1997), which is measured by the plasma instrument on *Voyager 2* (Wang et al. 2000; Wang & Richardson 2003).

The *Voyager* plasma instrument also measures the temperature of the core solar wind distribution. One infers from the observed properties of the termination shock and the insufficient heating in the core distribution across the shock (Richardson et al. 2008; Richardson & Stone 2009) that the core remains substantially distinct from the accumulating pickup protons throughout the supersonic solar wind. Nevertheless, significant ongoing heating of the core is found far from the Sun (Richardson et al. 1995; Richardson & Smith 2003). At distances of 40–80 AU, the only plausible source for this heating is some process that taps the large pool of energy residing in the interstellar pickup protons.

We have constructed a model of this heating that has had some success in reproducing the observed solar wind temperatures. The basic idea, as first presented by Williams et al. (1995), is that the waves generated through the scattering of new pickup protons to near isotropy feed into a turbulent cascade which is ultimately dissipated by heating the core protons. A phenomenological model of turbulent evolution was developed to follow the behavior of large-scale turbulent eddies in the radially expanding solar wind (Zank et al. 1996; Matthaeus et al. 1999b; Smith et al. 2001). The steady-state turbulence was assumed to be driven by shear and compressional motions in the inner heliosphere, and by the pickup proton fluctuations in the outer heliosphere. The turbulent fluctuations were taken to dissipate at the Kolmogorov rate and the dissipative energy increased the temperature of the core solar wind protons. The core heating predicted from this steady-state model followed the general trend of the *Voyager* observations. A more exact treatment of the pickup proton scattering and wave generation led to quantitative improvements in this agreement (Isenberg et al. 2003; Isenberg 2005). Most recently, the substantial variability of the solar wind plasma parameters, averaged over a solar rotation, was incorporated into the model to test the comparison even further (Smith et al. 2006).

In Smith et al. (2006), the steady-state model was repeatedly applied for each solar-rotation-averaged observation period at *Voyager 2*. Each *Voyager* period was matched to a corresponding earlier period at 1 AU, assuming advection of the solar wind plasma at constant speed between the two radial positions. The

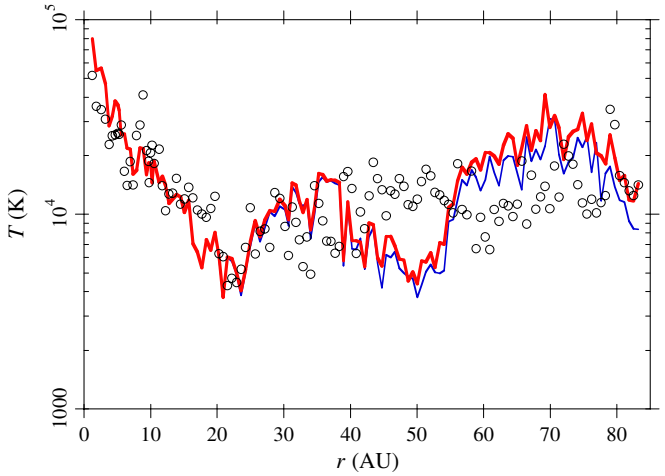

Figure 1. Comparison of model temperatures with observations at *Voyager 2* as functions of heliocentric radius. The circles are three-solar-rotation averages of the measured core solar wind temperature as *Voyager* moves away from the Sun. The thin blue line gives the model result when a constant solar wind speed is used, equivalent to the result in Smith et al. (2006). The thick red line gives the model result when the solar wind deceleration is taken into account. The two curves overlap almost completely for $r < 40$ AU.

average solar wind conditions from the National Space Science Data Center (NSSDC) Omnitape compilation at 1 AU were then used as input to the inner boundary of the model, which was propagated back out to the *Voyager* position. The variable input to the steady-state equations produced an effective response of the solar wind system to net changes on timescales of a solar rotation or longer. The average effect of shorter variations was still represented by the shear and compressional terms driving the turbulence. Core temperature results equivalent to those of Smith et al. (2006) are shown in Figure 1, where our use of three-solar-rotation time averages here is sufficient to illustrate the model.

The average temperatures in Figure 1 show that the model (thin blue line) and the *Voyager* data (circles) agree reasonably well inside 40 AU, but there are clear discrepancies beyond that point. The disagreement seen between $r = 40$ AU and 60 AU has been explained by Smith et al. (2006) as due to the latitudinal structure of the solar wind flow during solar minimum. *Voyager 2* travels to increasingly high latitude as it moves beyond 30 AU, and the well-organized structure of the wind during solar minimum means that the average solar wind parameters measured at Earth are not a good representation of the wind that reaches the spacecraft. We will justify this interpretation further in Section 3. (The thicker red line in Figure 1 will be discussed in Section 4.)

However, when *Voyager* passed 60 AU, solar maximum conditions had returned and it is more reasonable to assume that the Omnitape data provide valid input parameters for the model. During that time, the model predicted a core solar wind temperature which is about twice that measured at the spacecraft. It is important to ask what physically justifiable changes can be made to this model to lower the predicted temperature in this region.

Smith et al. (2006) considered several modifications in an effort to address this discrepancy. Various internal parameters that model the turbulent properties could be adjusted, but plausible new values either result in small differences in the distant temperature or in unacceptable disagreements with observations closer to the Sun. A smaller value of N_o can bring the model core temperature in line with the *Voyager* measurements, but only if this inflowing density is approximately halved. Such a low hydrogen density at the edge of the supersonic solar wind is not consistent with observations (Bzowski et al. 2009). Isenberg (2005) extended the earlier steady-state model to include the additional effect of second-order Fermi acceleration of the pickup protons, which would reduce the wave energy available to drive the turbulence. The consequent reduction in the model core temperature was also shown to be small. Finally, Ng et al. (2010) recently considered the consequences of replacing the Kolmogorov dissipation in the model with an Iroshnikov–Kraichnan formulation. Their initial results were encouraging, but more study is planned. We refer the reader to the cited papers for more detailed discussion of these efforts.

In this paper, we investigate the effect of including the deceleration of the solar wind which must accompany the pickup proton heating. The previous models took V_{sw} to be constant in r, but momentum loading from the pickup process requires the solar wind to slow down. The speed of a steady-state solar wind will fall linearly with heliocentric radius at large r (Holzer 1972; Isenberg 1986; Lee 1997), and this trend is seen in the *Voyager* data during solar maximum time periods. Incorporation of the solar wind slowdown is especially appealing in the context of the excess temperatures obtained in our model, since a lower energy per particle ($\sim V_{sw}^2$) in the initial ring beam would result. A lower initial energy could reduce the pickup proton driving of the turbulence, and thus lower the dissipative heating of the solar wind core.

However, in this paper we show that a decelerating solar wind leads to a hotter solar wind proton core, contrary to the above expectation. In the next section, we derive the modifications to the phenomenological turbulence model when the solar wind speed is not constant. Section 3 describes the specific deceleration resulting from the pickup of interstellar hydrogen. Section 4 gives the results of our model calculations when the solar wind deceleration is included, and explains this effect. In Section 5, we discuss these results and present our conclusions.

2. TURBULENT EVOLUTION MODEL WITH RADIALLY DEPENDENT SOLAR WIND SPEED

The evolution of solar wind turbulence can be described by a simplified phenomenological model which follows the intensity of the energy-containing eddies in a radially expanding steady solar wind (Zank et al. 1996; Matthaeus et al. 1999b; Smith et al. 2001, 2006; Isenberg et al. 2003; Isenberg 2005; Breech et al. 2008). These large-scale eddies are driven by sources due to compressions and shears in the inner heliosphere, and by pickup proton isotropization in the outer heliosphere. The turbulent energy is assumed to proceed to dissipative scales through a well-developed cascade, without specifying the details of the nonlinear couplings that actually transport the energy in the inertial range. These models are conceptually similar to the "engineering models" of hydrodynamical turbulence (Bradshaw et al. 1981), which originated in the pioneering work of von Kármán & Howarth (1938).

In these models, the turbulence is characterized by two quantities: $Z^2 = \langle \delta v^2 \rangle + \langle \delta b^2 / 4\pi\rho \rangle$, the turbulent intensity at the energy-containing scales in Elsässer units; and λ, the correlation length of the turbulent fluctuations. The cross helicity of the fluctuations is assumed here to be zero, appropriate for the equatorial region of the solar wind beyond $\sim$10 AU. Extensions of this model to include non-zero cross helicity have been

presented (Matthaeus et al. 2004; Breech et al. 2005, 2008), but will not be considered here.

To incorporate a spatially dependent solar wind speed into the phenomenological turbulent evolution model, we return to the earlier analysis of Zhou & Matthaeus (1990) and Matthaeus et al. (1996). The steady-state behavior of the turbulent intensity and the correlation length in a solar wind flow $V_{\rm sw}$ is described by

$$\boldsymbol{V}_{\rm sw}\cdot\boldsymbol{\nabla}Z^2+\left(\frac{\boldsymbol{\nabla}\cdot\boldsymbol{V}_{\rm sw}}{2}+M\sigma_D\right)Z^2=F_{\rm shear}+F_{\rm pickup}-\frac{\alpha Z^3}{\lambda} \tag{1}$$

$$\boldsymbol{V}_{\rm sw}\cdot\boldsymbol{\nabla}\lambda-M\sigma_D\lambda=G_{\rm shear}+G_{\rm pickup}+\beta Z. \tag{2}$$

The product $M\sigma_D$ represents the effects of mixing between the large-scale expansion of the solar wind flow and the small-scale fluctuations. Here, the mixing coefficient M is a geometry-dependent term coupling the spatial inhomogeneity and the turbulent motions (Breech et al. 2008), σ_D is the normalized energy difference between the kinetic and magnetic fluctuation components, $\sigma_D=(r_A-1)/(r_A+1)$, and r_A is the Alfvén ratio of these energies, $r_A=E_v/E_b$. The F and G terms represent the forcing effects on Z^2 and λ due to the turbulent sources of shear and pickup. The parameters α and β are set by considerations of local turbulence theory, where we choose $\alpha=2\beta$, corresponding to self-similar decay of the fluctuations (Hossain et al. 1995; Matthaeus et al. 1996).

In the supersonic region beyond 1 AU, we take the solar wind flow to expand spherically in the radial direction. We assume (Zank et al. 1996; Matthaeus et al. 1996, 1999b; Smith et al. 2001) that the turbulence is composed of transverse fluctuations which are uniformly distributed in the plane perpendicular to the average magnetic field direction. We then take that direction to be the Parker spiral angle, Ψ, where $\tan\Psi=B_\phi/B_r=r\Omega/V_{\rm sw}$, and Ω is the angular rotation frequency of the Sun. Under these assumptions, the mixing coefficient M becomes

$$M=\frac{V_{\rm sw}\cos^2\Psi}{r}-\frac{\cos 2\Psi}{2}\frac{dV_{\rm sw}}{dr}. \tag{3}$$

This result corrects the expression given in Zank et al. (1996), and is consistent with the formalism of Breech et al. (2008).

The forcing terms, F and G, are parameterized in the same manner as the earlier versions of this model, taking the compression and shear effects to fall as r^{-1}. We then obtain the equations

$$\frac{dZ^2}{dr}+\left(1+\sigma_D\cos^2\Psi\right)\frac{Z^2}{r}+\frac{1-\sigma_D\cos 2\Psi}{2}\frac{V'}{V_{\rm sw}}Z^2=C_{\rm sh}\frac{Z^2}{r}+\frac{Q}{V_{\rm sw}}-\frac{\alpha Z^3}{\lambda V_{\rm sw}} \tag{4}$$

$$\frac{d\lambda}{dr}-\sigma_D\left(\frac{\cos^2\Psi}{r}-\frac{\cos 2\Psi}{2}\frac{V'}{V_{\rm sw}}\right)\lambda=-\hat{C}_{\rm sh}\frac{\lambda}{r}-\frac{\beta}{\alpha}\frac{\lambda Q}{V_{\rm sw}Z^2}+\frac{\beta Z}{V_{\rm sw}}, \tag{5}$$

where $V'=dV_{\rm sw}/dr$, and Q is the fluctuation source due to the pickup proton isotropization. The pickup source is modeled as

$$Q=\zeta\frac{V_{\rm sw}^2}{n}\frac{dN}{dt}, \tag{6}$$

where n is the solar wind density, dN/dt is the rate at which new pickup protons are created, and ζ is the fraction of initial pickup proton energy which is given up in the isotropization process, generating new fluctuations which drive the turbulence.

These turbulent evolution equations are supplemented by an energy equation to yield heating of the core solar wind protons by the turbulent dissipation

$$\frac{dT}{dr}=-\frac{4}{3}\frac{T}{r}-\frac{2}{3}T\frac{V'}{V_{\rm sw}}+\frac{m}{3k_B}\frac{\alpha Z^3}{\lambda V_{\rm sw}}, \tag{7}$$

where m and T are the proton mass and core temperature, respectively, while k_B is the Boltzmann constant. This equation is identical to that used in the previous works, with the addition of the middle term on the right-hand side representing the adiabatic heating (or cooling) when the spherically symmetric solar wind flow speed changes with r.

The pickup proton-driven turbulent heating, given by the last term in Equation (7), increases with distance from the Sun and dominates the other effects beyond ~25 AU. The magnitude of the pickup proton source Q is determined by the details of the pitch-angle scattering of new pickup protons from their initial ring distribution in the azimuthal average spiral field to a closed shell distribution in velocity space. These details are parameterized by the coefficient ζ. In the initial models (Williams et al. 1995; Matthaeus et al. 1999a; Smith et al. 2001), the new pickup protons were assumed to scatter to a bispherical distribution (Galeev & Sagdeev 1988; Williams & Zank 1994), represented by $\zeta=V_A/V_{\rm sw}$ where V_A is the local Alfvén speed. The bispherical distribution, introduced in the context of the intense fluxes found in cometary pickup, corresponds to the velocity-space shell which results when pickup ions efficiently damp the resonant stable modes and only scatter through the interaction with the self-generated unstable waves. In the case of interstellar pickup protons, this assumption was shown to inject too much energy to the turbulent fluctuations, leading to solar wind temperatures far in excess of the observed values (Smith et al. 2001).

The revised analysis by Isenberg et al. (2003) and Isenberg (2005) recognized that the ionization that creates new interstellar pickup protons in the outer heliosphere is much slower than the expected rate for redistribution of wave energy by nonlinear turbulent processes. Thus, a power-law spectrum of dispersive ambient waves was taken to govern the scattering of the new pickup protons. The cyclotron–resonant interaction was modeled using the four parallel-propagating transverse wave modes, right or left circularly polarized, propagating in either direction along the magnetic field. The waves were described by the standard dispersion relation in a cold electron–proton plasma, with intensities proportional to $k^{-5/3}$ and equally distributed in all four modes. This "dominant turbulence" analysis resulted in particular shapes for the fully scattered pickup proton shells, which retained more energy in the particles than those of the bispherical distribution, reducing the energy available to drive the turbulence. Additional reductions were obtained by including the effect of non-resonant spreading of the initial pickup ring distribution due to the fluctuating field direction in the ambient turbulence (Isenberg 1996; Németh et al. 2000). The resulting energy partition coefficient, ζ, is a function of $V_A/V_{\rm sw}$ and of the non-resonant pitch-angle spread, denoted by Δ. This function yielded solar wind heating much closer to the observed values than the bispherical model. This partition function was then used by Smith et al. (2006) in the variable-input model shown in Figure 1. The details of this

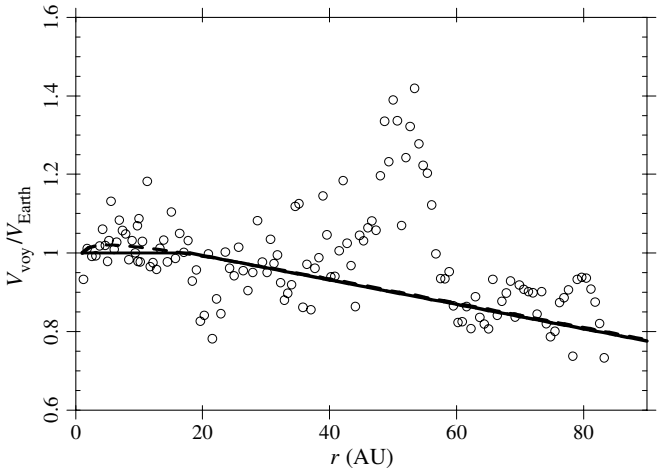

Figure 2. Deceleration of the solar wind. The circles show the ratio of the three-solar-rotation-averaged solar wind speed measured at *Voyager 2* to the time-shifted average speed measured at Earth obtained from the NSSDC Omnitape. The dashed line is obtained from the three-fluid pickup proton model of Isenberg (1986), and the solid line shows the deceleration assumed in this paper (Equation (8)).

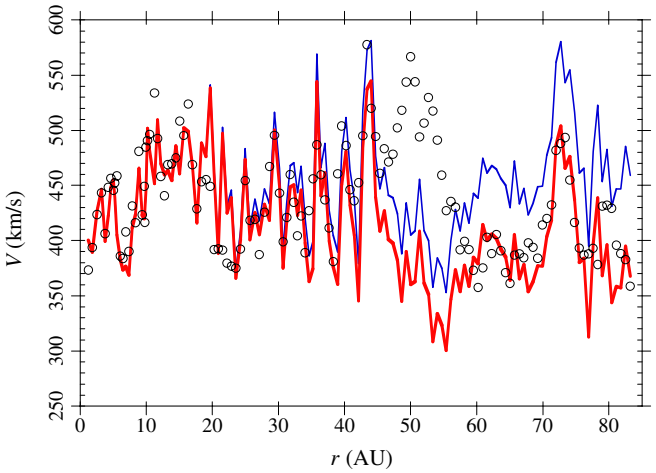

Figure 3. Comparison of predicted and measured solar wind speed. The circles are the three-solar-rotation-averaged measurements of solar wind speed at *Voyager 2*. The thin blue line shows the prediction using constant wind speed to track back to 1 AU, and then out again to *Voyager*. The thick red line shows the prediction when the deceleration (8) is used instead.

dispersive, dominant turbulence function ζ are given in Isenberg (2005).

3. SOLAR WIND DECELERATION DUE TO INTERSTELLAR PICKUP PROTONS

The decrease in solar wind speed by the momentum loading of the interstellar pickup protons can be clearly seen in Figure 2. The circles are the solar wind speeds measured at *Voyager 2*, averaged over three solar rotations, divided by the averaged, time-shifted speed measured at 1 AU from the NSSDC Omnitape data. In this single figure, the time shift between *Voyager 2* and 1 AU is calculated by taking the observed average wind speed at *Voyager* to be a constant, as in Smith et al. (2006). This procedure neglects the slight effect of the radial deceleration on the choice of the appropriate Omnitape time period. In all the analysis to follow, this deceleration will be included in the determination of the time shift.

The large relative speeds found between 40 and 55 AU occurred during solar minimum, when the interplanetary magnetic field was highly organized in heliolatitude. During this time, the solar wind seen at the high-latitude position of *Voyager 2* is not well related to the equatorial wind at Earth. Conversely, we see that three-rotation averages of solar wind speed during the remaining time periods are reasonably well correlated over the latitude difference between *Voyager 2* and Earth, implying that our purely radial model is justified in taking the Omnitape data for its inner boundary condition.

The dashed line in Figure 2 is the speed ratio obtained from the three-fluid model of Isenberg (1986), taking $V_{sw} = 450$ km s^{-1} at 1 AU, the inflowing hydrogen density $N_o = 0.1$ cm^{-3}, and a proton ionization rate at 1 AU $\nu_o = 7.5 \times 10^{-7}$ s^{-1}leading to an ionization cavity radius of $L = 5.6$ AU in the upwind direction. These values and the resulting speeds are consistent with similar findings by Wang & Richardson (2003).

We represent this deceleration in the turbulent heating model of this paper by taking the functional form

$$\begin{aligned} V_{sw}(r) &= V_{1AU} - 1.4(r - 18) \quad r \geqslant 18 \text{ AU} \\ &= V_{1AU} \qquad\qquad\qquad\quad r < 18 \text{ AU}, \end{aligned} \tag{8}$$

where V_{sw} and V_{1AU} are in units of km s^{-1} and r is in units of AU. The dependence (8) is shown in Figure 2 by the solid line. Figure 3 shows the three-solar-rotation-averaged solar wind speed measured at *Voyager 2*, compared to the predicted speed using Equation (8) to obtain the time-shifted values of V_{1AU}. Apart from the period of solar minimum, the agreement is very good.

4. MODEL RESULTS

We repeatedly integrate the model equations (4)–(7) in r from 1 AU out to the three-solar-rotation-averaged position of *Voyager 2*, using the time-shifted three-solar-rotation-averaged solar wind conditions at 1 AU from the NSSDC Omnitape as input boundary values for the model. Here, and in all the following analysis, the deceleration (8) is included in the calculation of the time shift. Since we are primarily interested in the heating from the pickup protons, taking place beyond 10 AU, we assume in our model that the average magnetic field is azimuthal, $\Psi = \pi/2$, and that the Alfvén ratio is a constant at $r_A = 1/2$ (Roberts et al. 1987). Finally, we take $C_{sh} = 1.4$, $\hat{C}_{sh} = 0.1$, $\alpha = 0.8$, and $\beta = 0.4$, roughly consistent with the parameter choices of Breech et al. (2008).

In Figure 4, we show the model results for the fluctuating intensity of one transverse component of the magnetic field,

$$\langle \delta B_N^2 \rangle = \frac{2\pi\rho}{1 + r_A} Z^2, \tag{9}$$

and the correlation length, λ, along with the corresponding values obtained from analyzing the *Voyager* observations, shown as circles.

The *Voyager* magnetic field data are obtained from the NSSDC and the variance of the N-component (in the standard R, T, N heliospherical coordinate system) is computed over 10 hr intervals. These variances are then averaged over 0.5 AU, which provides greater smoothing than the values presented in Smith et al. (2006). *Voyager*/MAG data are available out to and beyond the termination shock, but we limit this analysis to observations prior to the shock crossing at $r = 84$ AU. *Voyager*/PLS observations are analyzed in a similar manner using different codes with secondary averages over three solar rotations rather

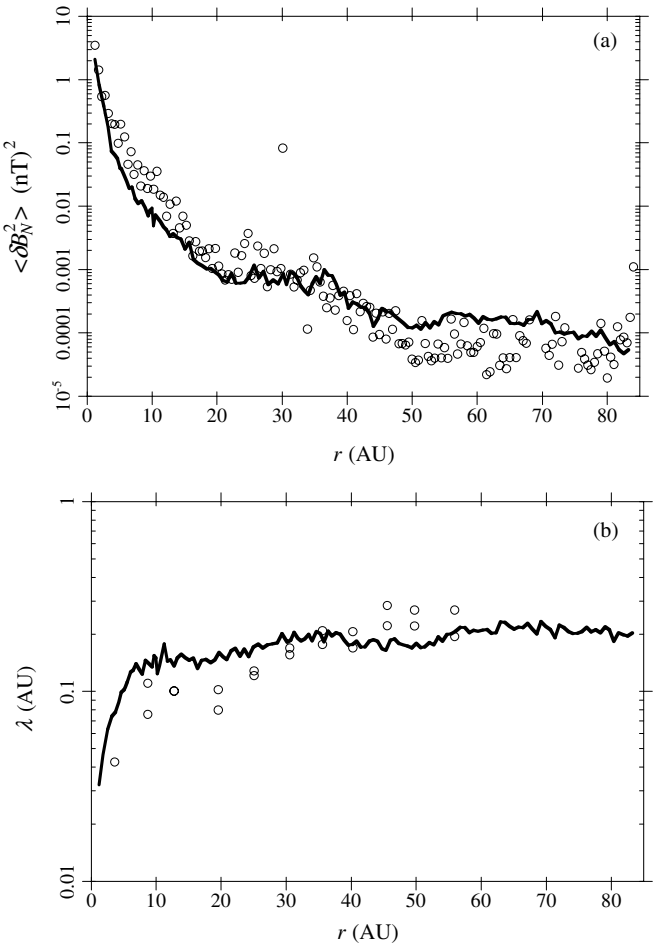

Figure 4. (a) Fluctuation intensity of the N-component of the magnetic field. The circles are the three-solar-rotation averages of the measurements at *Voyager 2*. The solid line shows the model results. (b) Turbulence correlation length. The circles are the results of analyzing the *Voyager 2* magnetometer data, using two different techniques with 120 hr maximum lags, averaged over 5 AU. The solid line shows the model results.

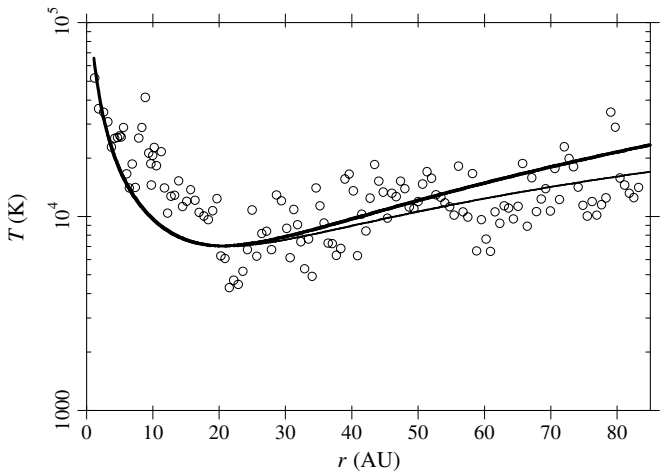

Figure 5. Comparison of temperatures from a constant input model. The thin line uses constant solar wind speed, and the thick line uses the decelerating solar wind. The circles are the *Voyager* temperatures as in Figure 1, and are shown here for reference.

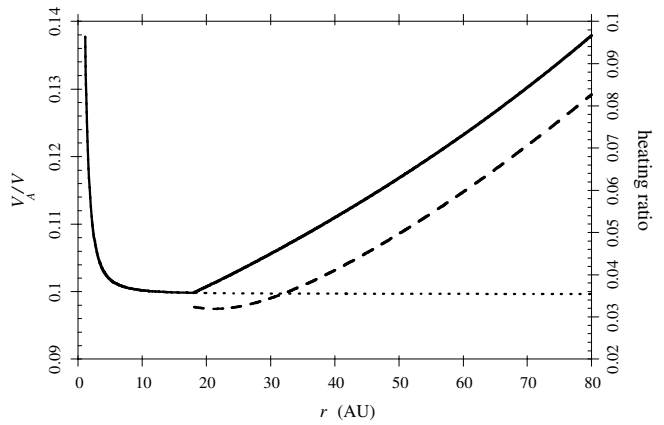

Figure 6. Model parameters for the constant input models of Figure 5. The solid line shows the value of V_A/V_{sw} as a function of radius for the decelerating model, while the dotted line comes from the solution with constant solar wind speed. The dashed line, using the scale on the right, shows the ratio of the adiabatic heating to the turbulent dissipation heating driven by pickup protons (second and third terms, respectively, in Equation (7)) in the decelerating case.

than 0.5 AU. This accounts for the greater fluctuation level in the temperature plots. Values for the correlation length of the fluctuations are computed using either the integration or the e-folding definition of this length, as described in Smith et al. (2001), and both are shown in Figure 4(b). The correlation length analysis uses 120 hr maximum lag, and these values are then averaged over 5 AU. This analysis was limited to $r < 56$ AU due to frequent data gaps beyond that distance.

The model core proton temperature results using the decelerating solar wind (8) are given by the thick red line in Figure 1, while the thin blue line shows the results using a constant solar wind speed, V_{1AU}, for each *Voyager* point. These results exhibit an increased proton temperature when the solar wind deceleration is included, contrary to the expectation of lower input energy from pickup. The temperature increase is more clearly illustrated using steady input conditions at 1 AU. Figure 5 shows the model temperatures with (thick line) and without (thin line) deceleration for constant 1 AU input values of $V_{sw} = 450\,\mathrm{km\,s^{-1}}$, $V_A = 65$ km s^{-1}, $Z^2 = 700$ (km s^{-1})^2, $\lambda = 0.027$ AU, and $T = 7 \times 10^4$ K. The larger temperature for decelerating wind is evident.

We find that this behavior is due to the sensitive dependence of the partition function ζ on the value of V_A/V_{sw}, which overcomes the effect of smaller pickup energy per particle in slower wind. This effect is amplified by the fact that, in the azimuthal field of the outer heliosphere, a decelerating solar wind leads to an increasing Alfvén speed. In steady state we have $BV_{sw}r = $ constant and $nV_{sw}r^2 = $ constant, so $V_A \sim V_{sw}^{-1/2}$ and $V_A/V_{sw} \sim V_{sw}^{-3/2}$. Figure 6 shows the value of V_A/V_{sw} as a function of r for the steady input solutions in Figure 5. The dotted line corresponds to the constant speed model, and the solid line shows the decelerating model. We see that the value of this parameter rises sharply for $r > 18$ AU in the decelerating wind, leading to increased energy transferred to the fluctuations from isotropizing the pickup protons.

Of course, a decelerating flow will also be heated by adiabatic compression, given by the second term on the right-hand side of Equation (7). However, we find that the dominant effect here is the increased turbulent driving by the pickup proton scattering. The dashed curve in Figure 6 shows the ratio of the second and third terms of the right-hand side of Equation (7) for the decelerating steady input solution of Figure 5, and it is seen that the compressional heating is less than 10% of the turbulent dissipative heating.

5. DISCUSSION AND CONCLUSIONS

In this paper, we have extended our model of turbulent heating driven by pickup of interstellar hydrogen in the outer heliosphere to include the effect of the solar wind deceleration which must accompany the pickup. One motivation for this step was to see if pickup in the slower wind would reduce the model solar wind temperatures to agree with the *Voyager 2* data beyond 60 AU. However, we found that the larger values of V_A/V_{sw} produced by the deceleration cause enough of an increase in the energy partition function ζ to overcome the reduction in the energy/particle due to the factor of V_{sw}^2. Thus, the energy added to the model turbulence actually increases in the decelerating wind, leading to hotter temperatures.

Consequently, we are still seeking possible changes in this model to improve the predictions of core proton temperatures in the outer heliosphere. Several obvious mechanisms remain to be considered, even within the context of this turbulent evolution picture. For instance, our model currently places all the dissipative energy into heating the core protons. However, if a substantial fraction of this energy were to heat electrons instead (Breech et al. 2009; Cranmer et al. 2010), there could be better agreement in the proton core temperatures.

Another possible improvement follows from recognizing that the pickup proton driving appears in quasi-parallel propagating waves, while the turbulence formalism used here is really appropriate to two-dimensional quasi-perpendicular fluctuations. Such an improved model is being developed along these lines by Oughton and colleagues (Oughton et al. 2006, 2010). This "two-component" model describes the evolution of distinct, but interacting, fluctuating fields: a quasi-two-dimensional turbulent field and a separate "wave-like" field with different phenomenological couplings. We are presently investigating the predictions of this model for describing the observed solar wind properties in the outer heliosphere.

We thank the *Voyager*/MAG team for data used in this study. We are also grateful for valuable conversations with E. Möbius and S. Oughton. P.A.I. and C.W.S. were supported in part by NSF grant ATM 0635863 and NASA Guest Investigator grants NNX07AH75G and NNX08AJ19G. C.W.S. was further supported by Caltech subcontract 44A1085631 for the *ACE*/MAG instrument that contributes to the Omni data set. W.H.M. was supported by NASA grant NNX08A147G, and J.D.R. was supported under NASA contract 959203 from JPL to MIT.

REFERENCES

Bogdan, T. J., Lee, M. A., & Schneider, P. 1991, J. Geophys. Res., 96, 161
Bradshaw, P., Cebeci, T., & Whitelaw, J. H. 1981, Engineering Calculation Methods for Turbulent Flow (San Diego, CA: Academic)
Breech, B., Matthaeus, W. H., Cranmer, S. R., Kasper, J. C., & Oughton, S. 2009, J. Geophys. Res., 114, A09103
Breech, B., Matthaeus, W. H., Minnie, J., Bieber, J. W., Oughton, S., Smith, C. W., & Isenberg, P. 2008, J. Geophys. Res., 113, A08105
Breech, B., Matthaeus, W. H., Minnie, J., Oughton, S., Parhi, S., & Bieber, J. W. 2005, Geophys. Res. Lett., 32, L06103
Bzowski, M., Möbius, E., Tarnopolski, S., Izmodenov, V., & Gloeckler, G. 2009, Space Sci. Rev., 143, 177
Cranmer, S. R., Matthaeus, W. H., Breech, B. A., & Kasper, J. C. 2010, ApJ, 702, 1604
Galeev, A. A., & Sagdeev, R. Z. 1988, Ap&SS, 144, 427
Gloeckler, G., Fisk, L. A., & Geiss, J. 1997, Nature, 386, 374
Holzer, T. E. 1972, J. Geophys. Res., 77, 5407
Hossain, M., Gray, P. C., Pontius, D. H., Matthaeus, W. H., & Oughton, S. 1995, Phys. Fluids, 7, 2886
Isenberg, P. A. 1986, J. Geophys. Res., 91, 9965
Isenberg, P. A. 1996, in AIP Conf. Proc. 382, Solar Wind Eight, ed. D. Winterhalter et al. (Melville, NY: AIP), 626
Isenberg, P. A. 2005, ApJ, 623, 502
Isenberg, P. A., Smith, C. W., & Matthaeus, W. H. 2003, ApJ, 592, 564
Lee, M. A. 1997, in Cosmic Winds and the Heliosphere, ed. J. R. Jokipii, C. P. Sonett, & M. S. Giampapa (Tucson, AZ: Univ. Arizona Press), 857
Lee, M. A., & Ip, W.-H. 1987, J. Geophys. Res., 92, 11041
Matthaeus, W. H., Minnie, J., Breech, B., Parhi, S., Bieber, J. W., & Oughton, S. 2004, Geophys. Res. Lett., 31, L12803
Matthaeus, W. H., Smith, C. W., & Bieber, J. W. 1999a, in AIP Conf. Proc. 382, Solar Wind Nine, ed. S. R. Habbal et al. (Melville, NY: AIP), 511
Matthaeus, W. H., Zank, G. P., & Oughton, S. 1996, J. Plasma Phys., 56, 659
Matthaeus, W. H., Zank, G. P., Smith, C. W., & Oughton, S. 1999b, Phys. Rev. Lett., 82, 3444
Németh, Z., Erdös, G., & Balogh, A. 2000, Geophys. Res. Lett., 27, 2793
Ng, C. S., Bhattacharjee, A., Munsi, D., Isenberg, P. A., & Smith, C. W. 2010, J. Geophys. Res., 115, A02101
Oughton, S., Dmitruk, P., & Matthaeus, W. H. 2006, Phys. Plasmas, 13, 042306
Oughton, S., Matthaeus, W. H., Smith, C. W., & Breech, B. 2010, in AIP Conf. Proc. 1216, Solar Wind 12, ed. M. Maksimovic et al. (Melville, NY: AIP), 210
Richardson, J. D., Kasper, J. C., Wang, C., Belcher, J. W., & Lazarus, A. J. 2008, Nature, 454, 63
Richardson, J. D., Paularena, K. I., Lazarus, A. J., & Belcher, J. W. 1995, Geophys. Res. Lett., 22, 325
Richardson, J. D., & Smith, C. W. 2003, Geophys. Res. Lett., 30, 10
Richardson, J. D., & Stone, E. C. 2009, Space Sci. Rev., 143, 7
Roberts, D. A., Klein, L. W., Goldstein, M. L., & Matthaeus, W. H. 1987, J. Geophys. Res., 92, 11021
Smith, C. W., Isenberg, P. A., Matthaeus, W. H., & Richardson, J. D. 2006, ApJ, 638, 508
Smith, C. W., Matthaeus, W. H., Zank, G. P., Ness, N. F., Oughton, S., & Richardson, J. D. 2001, J. Geophys. Res., 106, 8253
von Kármán, T., & Howarth, L. 1938, Proc. R. Soc. A, 164, 192
Wallis, M. 1971, Nature, 233, 23
Wang, C., & Richardson, J. D. 2003, J. Geophys. Res., 108, 1058
Wang, C., Richardson, J. D., & Gosling, J. T. 2000, Geophys. Res. Lett., 27, 2429
Williams, L. L., & Zank, G. P. 1994, J. Geophys. Res., 99, 19229
Williams, L. L., Zank, G. P., & Matthaeus, W. H. 1995, J. Geophys. Res., 100, 17059
Wu, C. S., & Davidson, R. C. 1972, J. Geophys. Res., 77, 5399
Zank, G. P. 1999, Space Sci. Rev., 89, 413
Zank, G. P., Matthaeus, W. H., & Smith, C. W. 1996, J. Geophys. Res., 101, 17093
Zhou, Y., & Matthaeus, W. H. 1990, J. Geophys. Res., 95, 10291